Mineralogy and Petrology (1999) 67: 143–161

Mineralogy and Petrology

Cryptic metasomatism in the upper mantle beneath Southeastern Austria: a laser ablation microprobe-ICP-MS study

G. Dobosi[1,*], **G. Kurat**[2], **G. A. Jenner**[1], and **F. Brandstätter**[2]

[1] Department of Earth Sciences, Memorial University of Newfoundland, St. John's, Newfoundland, Canada
[2] Mineralogisch-Petrographische Abteilung, Naturhistorisches Museum Wien, Wien, Austria

With 5 Figures

Received December 11, 1998;
revised version accepted April 14, 1999

Summary

Upper mantle xenoliths from the classical location, Kapfenstein, Styria, as well as from Fehring, Styria, and Tobaj, Burgenland, have been analyzed by laser ablation microprobe inductively-coupled plasma mass spectrometry (LAM-ICP-MS). At all locations spinel lherzolite is the predominant xenolith type and thus our sample contains nine spinel lherzolites and only one harzburgite (from the richest location, Kapfenstein, sample Ka 167). All the rocks have protogranular to protogranular – porphyroclastic transitional textures. Mineral compositions are typical for fertile upper mantle rocks with 0.89 ⟨mg⟩ 0.92 for silicates and 0.10 ⟨cr⟩ 0.12 for spinel (0.18 for the harzburgite). The minerals are equilibrated with respect to major, minor and trace elements, except for clinopyroxenes in the sample from Tobaj (To 100) and one sample from Fehring (Feh 002) which have variable incompatible trace element contents.

Trace element abundances are highest in clinopyroxene (3–4 × primitive mantle rare earth element – REEs – abundances) followed by orthopyroxene (about 0.5 × mantle REEs) and olivine (0.0005–0.05 × mantle REEs). Abundances of trace elements in all phases are usually correlated with their compatibility. The most incompatible elements (e.g., U, Th, Nb, Ta, La, Ce) are depleted with respect to the more compatible elements in three samples from Fehring and two from Kapfenstein. The remaining samples are enriched in either U, or U and Th, or the most incompatible REEs as

*Present address: Laboratory for Geochemical Research, Hungarian Academy of Sciences, Budaörsi út 45, H-1112 Budapest, Hungary

compared to Nb and Ta which are usually depleted with respect to less incompatible elements. Clinopyroxenes of the sample from Tobaj (To 100) and one sample from Fehring (Feh 002) have variable U, Th, Nb and Ta contents. In sample Feh 002 this variation is accompanied by a correlated variation of the light REE contents and their abundances are also correlated with the closeness to the surface. The enrichments in U and Th are, however, not accompanied by any significant enrichment in Nb and Ta, the concentrations of which stay at low levels.

The non-equilibrium trace element distribution in clinopyroxenes suggests that the metasomatic events took place shortly before the rocks were delivered to the Earth's surface. Thus, metasomatism and volcanic activity seem to be related and a consequence of the rising diapir underneath the Pannonian Basin. Several metasomatic events probably related to fluids dominated by CO_2, water, or both were taking place. However, the intensity of that activity was generally low, as was the tectonic activity in the border zone of the Pannonian Basin. Only harzburgite Ka 167 provides evidence for some elevated activity of depletion and enrichment processes comparable to what has been found in the central region of the basin.

Zusammenfassung

Kryptische Metasomatose im Oberen Erdmantel unterhalb Südost-Österreich: eine Studie mittels Laser-Ablations-Mikrosonde-ICP-MS

Erdmantel-Xenolithe vom klassischen Vorkommen in Kapfenstein, Steiermark, und von Fehring, Steiermark, und Tobaj, Burgenland, wurden mittels Laser-Ablations-Mikrosonde-induktiv gekoppeltes Plasma-Massenspektrometer (LAM-ICP-MS) analysiert. An allen Lokalitäten dominieren Spinell-Lherzolithe die Xenolith – Population. Unsere Proben umfassen daher neun Spinell-Lherzolithe und nur einen Harzburgit (von der an Xenolithen reichsten Lokalität, Kapfenstein, Probe Ka 167). Alle Gesteine haben protogranulare bis protogranular-porphyroklastische Textur. Die Mineral-Zusammensetzungen sind typisch für fertile Gesteine aus dem Oberen Erdmantel mit 0,89 ⟨mg⟩ 0,92 in den Silikaten und 0,10 ⟨cr⟩ 0,12 im Spinell (0,18 im Harzburgit). Die Minerale sind hinsichtlich Haupt-, Neben- und Spurenelement-Verteilung im Gleichgewicht, ausgenommen die Klinopyroxene in der Probe von Tobay (To 100) und einer Probe von Fehring (Feh 002). Diese haben variable Gehalte an inkompatiblen Spurenelementen.

Klinopyroxene haben die höchsten Spurenelement-Gehalte (3–4-fache Seltene-Erden-Element (SEE)-Gehalte des primitiven Erdmantels) gefolgt von Orthopyroxen (etwa 0,5-fache Erdmantel SEE) und Olivin (0,0005–0,005-fache Erdmantel SEE). Spurenelement-Häufigkeiten in allen Phasen sind üblicherweise mit ihrer Kompatibilität korreliert. In drei Proben von Fehring und zwei von Kapfenstein sind die inkompatibelsten Elemente (wie U, Th, Nb, Ta, La, Ce) gegenüber den etwas kompatibleren Elementen verarmt. Die übrigen Gesteine sind entweder an U, oder U und Th, oder den inkompatibelsten SEE relativ zu Nb und Ta angereichert. Die Letzteren sind üblicherweise relativ zu den weniger inkompatiblen Elementen verarmt. Klinopyroxene in der Probe von Tabaj (To 100) und einer Probe von Fehring (Feh 002) haben variable Gehalte an U, Th, Nb und Ta. Diese Variabilität ist in der Probe Feh 002 korreliert mit jener der Gehalte an leichten SEE und die Elementhäufigkeiten sind zusätzlich korreliert mit der Nähe zur Kornoberfläche. Die Anreicherungen an U und Th sind allerdings nicht von merklichen Anreicherungen an Nb und Ta begleitet, deren Häufigkeiten niedrig bleiben. Die unequilibrierte Spurenelementverteilung in den Klinopyroxenen deutet darauf hin, daß die Metasomatose kurz vor dem Transport der

Gesteine an die Erdoberfläche stattfand. Metasomatose und vulkanische Aktivität scheinen daher verbunden und eine Konsequenz des unterhalb des Pannonischen Beckens aufsteigenden Erdmantel-Diapirs zu sein. Mehrere metasomatische Aktivitäten durch Fluide dominiert von CO_2, Wasser, oder beiden sind erkennbar. Die Intensität der Ereignisse war allerdings gering, vergleichbar der geringen tektonischen Aktivität in der Grenzzone des Pannonischen Beckens. Nur der Harzburgit Ka 167 zeigt Spuren intensiver Verarmungs- und Anreicherungs-Prozesse, die vergleichbar sind jenen, welche in der zentralen Region des Beckens die Erdmantel-Gesteine geprägt haben.

Introduction

Knowledge of the trace element distribution in upper mantle xenoliths is essential for the understanding of the evolution of the lithospheric mantle and to trace the various depletion and enrichment processes which continuously modify its composition. However, while the rare earth element (REE), Sr and Zr contents of upper mantle peridotites are relatively well known, considerable less information is available on highly incompatible trace elements like U, Th, Nb or Ta. These elements have very low abundances in peridotites which can easily be affected by contamination during their transport to the surface and during their storage in the volcanic rock. *In situ* analysis of the abundances of these elements in minerals of peridotites instead of analyzing the bulk peridotite for trace elements is a possible way to avoid the effects of contamination. Moreover, *in situ* trace element analysis may reveal homogeneous or inhomogeneous distribution of the trace elements between and in the peridotitic minerals which gives information on attempted equilibration through diffusion during various stages of metasomatic changes. The development of a relatively new in situ analytical technique, the laser ablation microprobe-inductively coupled plasma-mass spectrometry (LAM-ICP-MS) is a powerful tool for the accurate analysis of trace elements with very low abundances with good spatial resolution.

In this paper we present LAM-ICP-MS trace element data (including not only the routinely determined REE and HFSE elements, but the rarely analyzed U, Th, Nb, Ta and Hf, as well) for clinopyroxene, orthopyroxene and olivine of mostly anhydrous spinel peridotite xenoliths from the Graz Basin, southeastern Austria.

Geological background and sample description

The Pannonian Basin is a Tertiary extensional back-arc basin in Eastern Central Europe surrounded by the Eastern Alps and the Carpathian fold belt (Fig. 1). Extension-related alkali basaltic volcanism occurred in several regions of the Basin predominantly during the Pliocene, closely following the Eocene to Pliocene subduction-related calc-alkaline volcanism (*Salters* et al., 1988; *Embey-Isztin* et al., 1993; *Embey-Isztin* and *Dobosi*, 1995; *Embey-Isztin* and *Kurat*, 1996). One of these alkali basalt provinces is the Graz Basin in southeastern Austria which is situated in the westernmost edge of the Pannonian Basin (Fig. 1) and comprises several outcrops (lava domes and tuff cones) of alkali basaltic rocks varying from basanites to nephelinites (*Heritsch*, 1967). The age of the volcanism in this area is 2.5–1.5 Ma (*Balogh* et al., 1994).

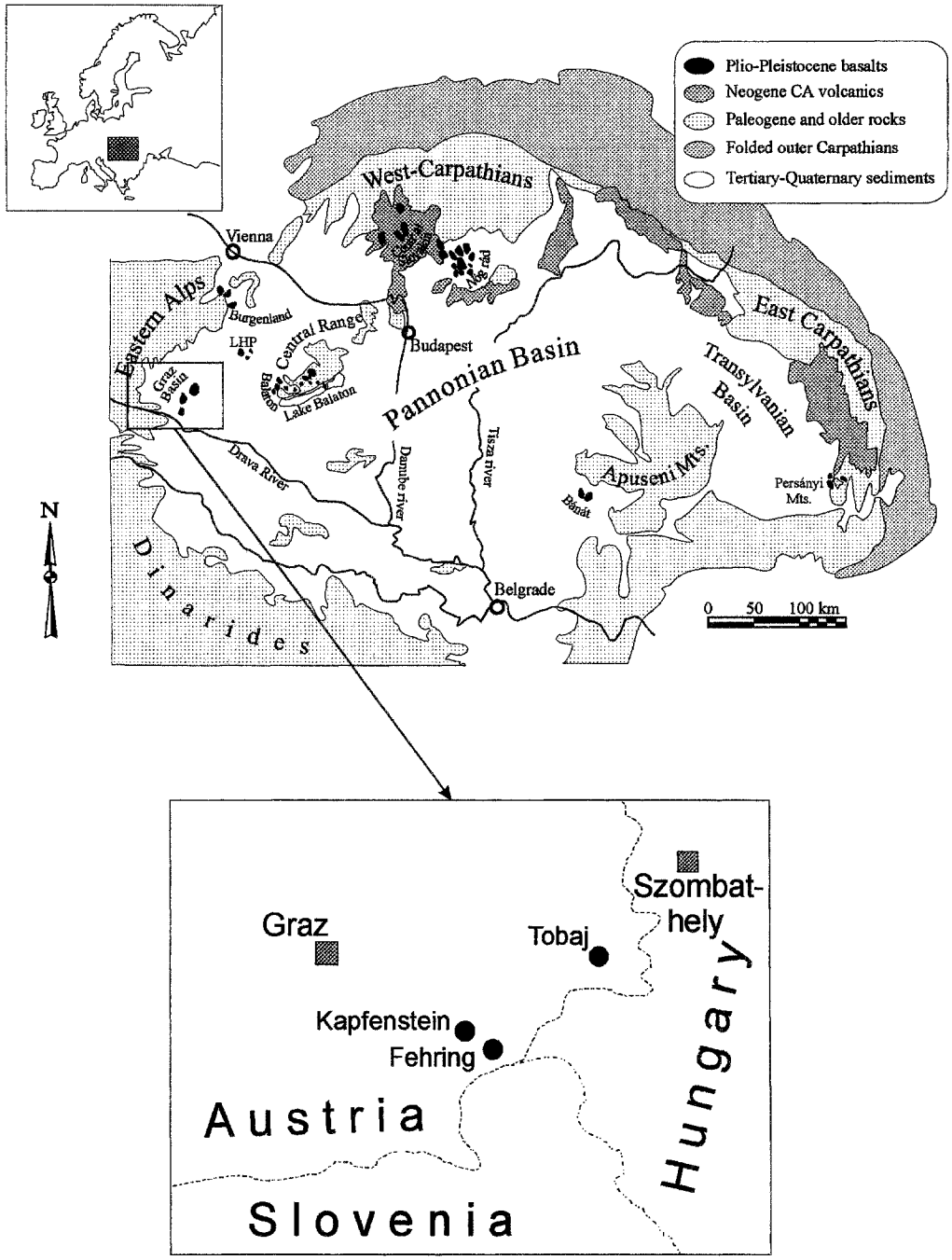

Fig. 1. Geological sketch map of the Pannonian Basin and the upper mantle xenolith localities of the Graz Basin, eastern Austria

Ultramafic xenoliths can be found mainly in the basaltic tuffs. In particular, the tuff of Kapfenstein (Fig. 1) contains abundant upper mantle lherzolites (*Kurat*, 1971; *Kurat* et al., 1980, 1991; *Vaselli* et al., 1996). Spinel peridotite xenoliths are also known from the tuff of Tobaj (*Richter*, 1971) and from the basaltic tuff near

the village of Fehring (Fig. 1). This latter locality is a newly discovered one whose upper mantle xenoliths have not been reported and investigated so far.

Ultramafic xenoliths analyzed in this study were collected from the volcanic tuffs of Kapfenstein, Tobaj and Fehring (labeled *Ka, To* and *Feh*, respectively). The xenolith samples from Kapfenstein are those investigated earlier by *Kurat* et al. (1980, 1991) and their detailed descriptions can be found in these reports. The sizes of xenoliths ranged from 5 cm to more than 20 cm in diameter (sample *Feh 001* is the largest one). The textures and mineralogical compositions of the xenoliths are rather monotonous: only protogranular or protogranular-porphyroclastic transitional types (as defined by *Mercier* and *Nicolas*, 1975) are present. The rocks are relatively coarse-grained with an average grain size of 1–2 mm. The roughly equidimensional grains have mostly curvilinear grain boundaries. Small scale, fine-grained recrystallization at grain boundaries, distorted clinopyroxene lamellae in orthopyroxene and kink bands in olivine suggest slight deformation.

All xenoliths belong to the Type I xenolith series as defined by *Frey* and *Prinz* (1978) and are spinel lherzolites, except for spinel harzburgite *Ka 167*. The lherzolites are composed of olivine (55–70 vol%), orthopyroxene (15–25%), clinopyroxene (10–15%) and spinel (few %). The harzburgite *Ka 167* contains significantly less clinopyroxene (about 2 vol%) and more olivine (around 83%) than the other samples.

Analytical methods

Microprobe analysis was carried out at the Natural History Museum of Vienna with an automated ARL-SEMQ electron microprobe equipped with crystal spectrometers and operated under conventional conditions (15 kV, 15 nA). The results are given in Table 1.

Trace element analyses of minerals were carried out by laser ablation microprobe – inductively coupled plasma – mass spectrometry (LAM-ICP-MS) available at Memorial University of Newfoundland. Hand-picked grains of clinopyroxene and orthopyroxene, olivine and spinel, (mounted in epoxy and polished) were analyzed. The laser ablation system used in this study is described in detail in *Jackson* et al. (1992), *Longerich* et al. (1993), *Jenner* et al. (1994) and *Fryer* et al. (1995). It consists of a Q-switched Nd: YAG laser operated at 266 nm in the ultraviolet region. The laser beam was focused onto the sample surface through the optics of a petrographic microscope. The pulse energy of the laser beam was 0.4–0.6 mJ, the diameter of the ablation pits were between 40 and 60 μm. The ablated material from the sample cell is carried by an Ar gas flow into the plasma torch of a Fisons VG PQ2+ ICP-MS instrument. Details of the ICP-MS analysis are given in *Horn* et al. (1997). All measurements were carried out using „time resolved analysis" data acquisition software operating in fast, peak-jumping mode. For the pyroxene analyses a spiked silicate glass (NIST 612) was used for calibration and Ca was used as an internal standard to correct the ablation yield differences between the individual analyses. For the analyses of olivine and spinel, BCR-2 glass was used for calibration and Mg was used as internal standard. Data reduction was made using the LAMTRACE© spreadsheet software written in-house by *S. Jackson*. All spot analyses were made on clean, inclusion- and crack-free areas of the grains, and 3 or 4

Table 1. *Major element composition of minerals in the Eastern Austrian peridotite xenoliths. Data for Ka 111, Ka 167 and Ka 168 are taken from* Kurat *et al. (1980); data for Ka 151 are from* Kurat *and* Embay-Isztin *(1991)*

	Feh 001	Feh 002	Feh 004	Feh 005	To 100	Ka 111	Ka 112	Ka 151	Ka 167	Ka 168
Clinopyroxene										
SiO_2	51.44	52.02	52.34	52.27	51.71	52.40	52.45	52.60	51.90	51.80
TiO_2	0.53	0.58	0.52	0.52	0.65	0.42	0.43	0.51	0.27	0.60
Al_2O_3	6.16	7.41	6.61	6.76	7.49	5.80	6.81	5.00	5.60	6.90
Cr_2O_3	1.06	0.93	1.19	0.88	0.99	0.81	1.12	0.90	1.06	0.79
FeO	2.56	2.97	2.42	2.58	2.86	3.00	2.66	2.86	2.67	2.76
MnO	0.12	0.10	0.10	0.07	0.09	0.09	0.10	0.10	0.09	0.11
MgO	14.75	14.97	15.05	14.80	14.33	15.90	15.35	16.90	16.30	15.80
CaO	21.83	21.03	22.17	21.79	21.21	19.80	20.83	20.20	19.90	20.10
Na_2O	1.23	1.35	1.17	1.20	1.61	1.38	1.42	0.82	1.44	1.60
total	99.68	101.37	101.56	100.88	100.93	99.60	101.17	99.89	99.23	100.46
Mg#	0.91	0.90	0.92	0.91	0.90	0.90	0.91	0.91	0.92	0.91
Orthopyroxene										
SiO_2	53.52	53.92	53.89	53.37	54.66	54.30	53.87	53.40	53.80	54.40
TiO_2	0.12	0.13	0.12	0.14	0.15	0.15	0.09	0.12	0.07	0.13
Al_2O_3	4.53	4.93	4.41	5.01	4.68	4.50	4.82	4.60	4.10	4.60
Cr_2O_3	0.52	0.43	0.45	0.43	0.36	0.42	0.41	0.42	0.53	0.37
FeO	5.93	6.46	6.14	6.08	6.34	6.10	6.06	5.80	5.80	6.10
MnO	0.14	0.15	0.15	0.13	0.15	0.12	0.15	0.13	0.13	0.15
MgO	33.22	33.27	33.22	32.96	32.80	33.60	32.76	33.30	34.00	33.90
CaO	0.65	0.77	0.65	0.63	0.71	0.78	0.79	0.87	0.78	0.74
Na_2O	0.05	0.09	0.03	0.06	0.06	0.11	0.12	0.11	0.11	0.10
total	98.67	100.13	99.07	98.81	99.91	100.08	99.07	98.75	99.32	100.49
Mg#	0.91	0.90	0.91	0.91	0.90	0.91	0.91	0.91	0.91	0.91
Olivine										
SiO_2	41.05	39.40	41.22	40.68	40.97	40.20	41.32	40.30	40.40	40.30
FeO	9.22	9.73	9.25	9.28	9.72	9.30	9.71	9.30	9.20	9.70
NiO	0.38	0.38	0.40	0.44	0.37	0.34	0.33	0.34		
MnO	0.14	0.15	0.08	0.16	0.11	0.13	0.12	0.13	0.12	0.11
MgO	49.82	48.74	50.09	48.12	49.55	48.40	49.43	49.10	49.70	49.40
CaO	0.04	0.04	0.05	0.05	0.07	0.08	0.09	0.08	0.06	0.07
total	100.65	98.44	101.09	98.74	100.80	98.45	101.00	99.25	99.48	99.58
Mg#	0.91	0.90	0.91	0.90	0.90	0.90	0.90	0.90	0.91	0.90
Spinel										
TiO_2	0.08	0.17	0.10	0.10	0.12	0.09	0.10	0.14	0.10	0.12
Al_2O_3	58.86	59.40	58.70	60.05	60.52	55.00	57.70	54.30	50.40	57.00
Cr_2O_3	12.10	10.52	12.14	10.62	10.25	11.10	13.89	10.90	16.10	9.30
FeO	7.78	7.52	7.49	7.33	7.21	12.40	6.83	11.20	11.30	11.10
MnO	0.15	0.18	0.14	0.10	0.10	0.12	0.06	0.10	0.13	0.11
MgO	21.03	21.95	20.93	21.50	21.43	21.10	20.99	21.80	20.40	21.30
total	100.31	99.94	99.80	100.02	99.91	99.81	99.77	98.44	98.43	98.93
Mg#	0.83	0.84	0.83	0.84	0.84	0.75	0.85	0.78	0.76	0.77
Cr#	0.12	0.11	0.12	0.11	0.10	0.12	0.14	0.12	0.18	0.10

grains of each mineral were analyzed at altogether 3 to 11 spots. The averaged results are reported in Table 2.

Typical detection limits under the conditions applied were 0.2–0.3 ppm for Sc and V, and between 0.01 and 0.001 ppm for Y, Sr, Zr, Nb, Hf, Ta and REEs. The accuracy of our LAM-ICP-MS analyses can be tested by comparing the results with those obtained with an ion microprobe on the same samples. Clinopyroxene

Table 2. *Trace element contents of the minerals in peridotite xenoliths. Data reported here are the averages of 6–10 individual spot analyses. Data for TiO_2 are in wt%; all other data are in ppm*

	Feh 001	Feh 002	Feh 004	Feh 005	To 100	Ka 111	Ka 112	Ka 151	Ka 167	Ka 168
Clinopyroxene										
Sc	77.8	69.9	77.2	72.8	77.1	67.1	74.6	74.2	64.7	70.1
TiO_2	0.63	0.65	0.63	0.65	0.74	0.64	0.52	0.51	0.29	0.70
V	261	282	256	264	279	245	259	256	253	256
Cr	5892	5291	6072	5046	5380	5259	6425	5477	7804	4752
Co	20.4	24.9	20.2	20.9	22.1	22.2	23.7	24.0	22.5	20.0
Ni	302	371	280	296	334	310	348	340	325	281
Sr	47.7	55.3	51.1	44.8	69.9	71.5	46.9	55.3	25.6	56.7
Y	16.8	16.8	17.4	18.5	18.1	15.8	15.2	15.1	10.7	15.8
Zr	26.8	23.6	26.9	22.3	32.6	24.9	17.7	18.4	5.5	24.0
Nb	0.13	0.17	0.16	0.11	0.17	0.17	0.30	0.43	1.10	0.09
La	0.77	1.82	0.81	0.67	0.90	1.09	0.42	0.73	2.39	0.77
Ce	3.03	4.61	3.07	2.77	3.95	4.21	2.08	2.59	6.14	3.65
Pr	0.64	0.72	0.65	0.57	0.77	0.73	0.47	0.47	0.46	0.70
Nd	3.75	3.89	4.00	3.69	4.43	4.01	2.99	2.74	1.12	3.94
Sm	1.65	1.64	1.72	1.64	1.84	1.68	1.37	1.26	0.52	1.63
Eu	0.69	0.72	0.72	0.71	0.78	0.71	0.59	0.57	0.27	0.71
Gd	2.33	2.30	2.47	2.47	2.51	2.18	1.99	1.85	1.10	2.14
Tb	0.45	0.45	0.47	0.49	0.49	0.43	0.40	0.40	0.24	0.43
Dy	3.14	3.13	3.31	3.42	3.44	2.98	2.81	2.75	1.88	2.96
Ho	0.68	0.68	0.70	0.75	0.73	0.66	0.62	0.61	0.44	0.65
Er	2.02	2.03	2.13	2.20	2.15	1.92	1.83	1.84	1.41	1.86
Tm	0.29	0.29	0.30	0.31	0.31	0.27	0.26	0.26	0.20	0.27
Yb	1.75	1.90	1.93	1.97	2.02	1.83	1.69	1.69	1.29	1.75
Lu	0.27	0.26	0.28	0.29	0.29	0.26	0.24	0.25	0.17	0.25
Hf	0.93	0.87	0.99	0.88	1.14	0.89	0.63	0.75	0.28	0.87
Ta	0.016	0.002	0.022	0.010	0.020	0.020	0.007	0.018	0.068	0.007
Th		0.32	0.013	0.010	0.022	0.012	0.014	0.040	0.051	
U		0.12	0.003		0.029	0.008		0.015	0.075	
Orthopyroxene										
Sc	23.9	20.9	22.8	22.7	22.1	22.1	21.4	22.7	2.8	21.7
TiO_2	0.15	0.15	0.15	0.17	0.17	0.17	0.13	0.14	0.09	0.18
V	109	101	104	116	109	101	101	110	97	112
Cr	2478	2306	2444	2594	2252	2173	3040	2588	3484	2229
Co	64.0	.68.5	67.3	72.1	73.8	65.1	67.3	71.6	63.9	75.2
Ni	753	825	760	630	884	680	792	830	760	716
Sr	0.064	0.146	0.100	0.063	0.116	0.182	0.131	0.193	0.070	0.123
Y	0.85	1.00	0.78	0.88	0.92	1.00	0.88	1.09	0.75	1.01
Zr	1.32	1.39	1.08	1.06	1.49	1.57	1.00	1.27	0.38	1.35
Nb	0.043	0.040	0.029	0.046	0.046	0.037	0.052	0.053	0.089	0.045
La	0.004	0.003	0.002	0.001		0.002		0.002	0.004	0.001
Ce	0.005	0.020	0.007	0.003	0.012	0.014	0.007	0.013	0.015	0.009
Pr	0.001	0.005	0.001	0.001	0.002	0.004	0.001	0.003	0.002	0.003
Nd		0.023	0.014	0.014	0.024	0.030	0.017	0.019	0.010	0.018
Sm	0.008	0.018	0.010	0.004	0.015	0.021	0.017	0.024	0.006	0.015
Eu	0.005	0.014	0.005	0.006	0.010	0.010	0.011	0.012	0.004	0.009
Gd	0.028	0.049	0.020	0.034	0.038	0.045	0.044	0.056	0.028	0.051
Tb	0.011	0.011	0.008	0.010	0.012	0.010	0.012	0.015	0.006	0.013
Dy	0.099	0.134	0.093	0.113	0.105	0.123	0.106	0.141	0.082	0.121
Ho	0.026	0.038	0.027	0.030	0.032	0.037	0.035	0.043	0.025	0.035
Er	0.122	0.155	0.127	0.120	0.121	0.157	0.140	0.156	0.113	0.155
Tm	0.027	0.030	0.022	0.027	0.026	0.027	0.026	0.032	0.019	0.031
Yb	0.252	0.222	0.222	0.254	0.267	0.251	0.211	0.271	0.198	0.255
Lu	0.044	0.041	0.042	0.051	0.044	0.045	0.041	0.051	0.036	0.048
Hf	0.044	0.055	0.036	0.054	0.053	0.049	0.036	0.049	0.014	0.040
Olivine										
Sc	3.11	3.32	2.90	2.86	2.95	3.83	3.86	4.37	4.20	3.46
TiO2	0.004	0.003	0.002	0.002	0.003	0.004	0.003	0.004	0.003	0.004
V	1.43	2.54	1.56	1.56	2.50	2.67	2.98	3.82	2.94	2.58
Cr	27.4	50.6	24.7	27.6	41.6	53.7	72.5	97.9	93.5	46.5
Co	138	134	136	133	145	138	139	136	136	146
Ni	2809	2743	2563	2406	2771	2415	2555	2644	2744	2432
Sr	0.012	0.009	0.019	0.019	0.022	0.010	0.004			0.004
Y	0.020	0.032	0.022	0.017	0.030	0.035	0.042	0.047	0.030	0.038
Zr	0.029		0.016	0.010	0.009	0.022	0.022	0.026	0.004	0.023
Nb	0.006	0.009	0.010			0.010		0.004	0.005	
Spinel										
TiO_2	0.06	0.13	0.08	0.07	0.11	0.10	0.13	0.12	0.09	0.13
V	350	373	395	355	299	332	390	314	392	344
Co	242	222	249	239	193	186	210	178	201	207
Ni	3011	3089	2905	3028	2852	2514	2671	2619	2431	2714

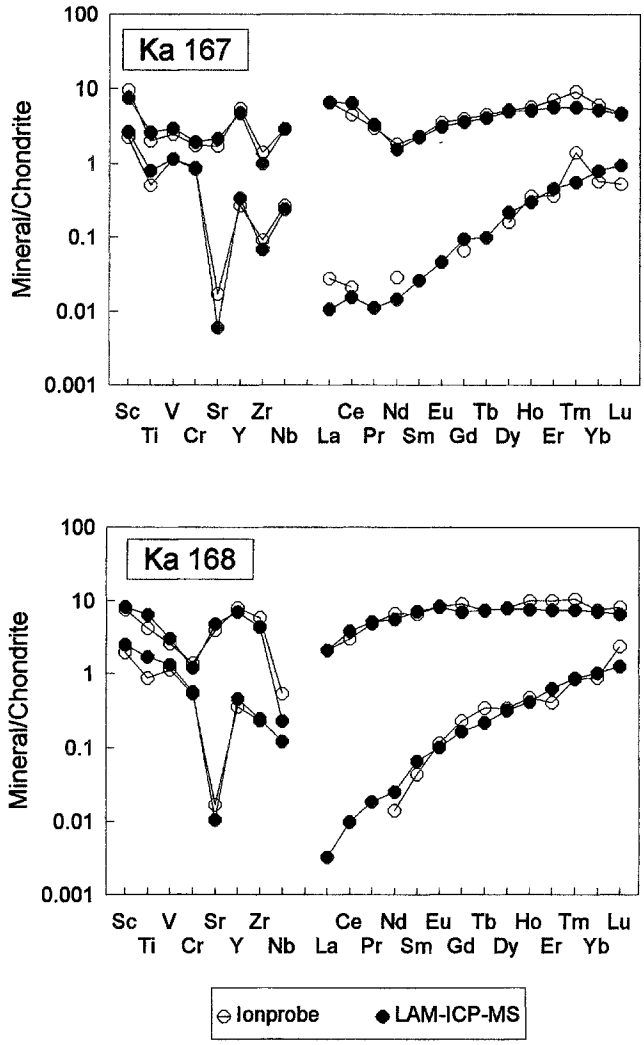

Fig. 2. Comparison of the chondrite-normalized trace element patterns of clinopyroxenes (high abundance) and orthopyroxenes (low abundance) of two upper mantle xenolithic peridotites from Kapfenstein (harzburgite Ka 167 and lherzolite Ka 168) analyzed by secondary ion mass spectrometry (SIMS, *P. Hoppe*, University of Bern) and by laser-ablation microprobe inductively-coupled plasma mass spectrometry (LAM-ICP-MS, this work). Chondrite data are from *Taylor* and *McLennan* (1985). Elements are arranged in order of increasing incompatibility, except for the REEs which are ordered by increasing Z

and orthopyroxene from samples *Ka 167* and *Ka 168* have been analyzed using the ion probe at the University of Bern, Switzerland (*P. Hoppe*, personal communication 1994). The comparison of the results (Fig. 2) shows good agreement between the data obtained by the two in situ methods.

Results

Major elements

All minerals are homogeneous with respect to their major element contents and have very uniform compositions throughout the whole xenolith suite (Table 1). Olivine has Mg-numbers (Fo-contents) between 0.89 and 0.91 and the abundance of minor elements (CaO 0.04–0.09 wt%; MnO 0.08–0.15 wt% and NiO 0.33–0.44 wt%) is very similar to those reported from other upper mantle rocks.

Orthopyroxene has an equal or slightly higher Mg-number than the coexisting olivine with all values lying between 0.90 to 0.91. The Al_2O_3 content is very similar in all samples (4.41–5.01 wt%); only the orthopyroxene from harzburgite *Ka 167* has a slightly lower Al_2O_3 content of 4.10 wt%. Kapfenstein orthopyroxenes have higher CaO contents (0.74–0.87 wt%) than those from the other localities (0.63–0.77 wt%).

The Mg-number of the clinopyroxenes is very similar to that of the coexisting olivine and orthopyroxene and varies between 0.90 and 0.92. The Al_2O_3 and Cr_2O_3 contents vary between 5.00 and 7.49 wt% and 0.79 and 1.19 wt%, respectively. Both elements have higher abundances of clinopyroxenes compared to orthopyroxenes. The CaO content of clinopyroxenes is lower in the Kapfenstein xenoliths (19.8–20.8 wt%) than in the xenoliths from Tobaj and Fehring (21.0–21.8 wt).

The spinels are also rather uniform in composition. They have high Mg-numbers around 0.75 and low Cr-numbers (atomic Cr/Cr+Al) between 0.10 and 0.12, except for harzburgite *Ka 167* whose spinel has a significantly higher Cr_2O_3 content (Cr-number = 0.18) than spinels of the other xenoliths.

Trace elements

The average trace element contents of clinopyroxenes, orthopyroxenes, olivines and spinels are presented in Table 2.

The primitive mantle-normalized trace element patterns of clinopyroxenes from the lherzolite samples are very similar to each other for most elements but differ significantly in the abundances of U, Th, Nb and Ta (Fig. 3). The medium and heavy REEs (from Sm to Lu) and Y show a smooth pattern at a level of approximately 3–4 times primitive mantle abundances and a slight decrease in the abundances from Nd toward La is evident. A weak negative anomaly for Ti and Zr and a slight positive anomaly for Sr is present in almost all clinopyroxenes. Clinopyroxenes are generally homogeneous with respect to their trace element contents, except for samples *Feh 002* and *To 100*. In *Feh 002* clinopyroxene, the light REEs (LREEs), especially La and Ce, show significant variation from depleted to slightly enriched patterns. Trace element zoning was not investigated systematically. However, a few clinopyroxene grains which were analyzed on two or three spots indicate that the marginal parts of the crystals are enriched in LREEs relative to the central regions.

The primitive mantle-normalized abundances of Nb and Ta are significantly lower than those of the LREEs (Fig. 3). They generally have abundances around 0.2–0.6 times primitive mantle which correspond to contents of Nb = 0.09–0.43 ppm

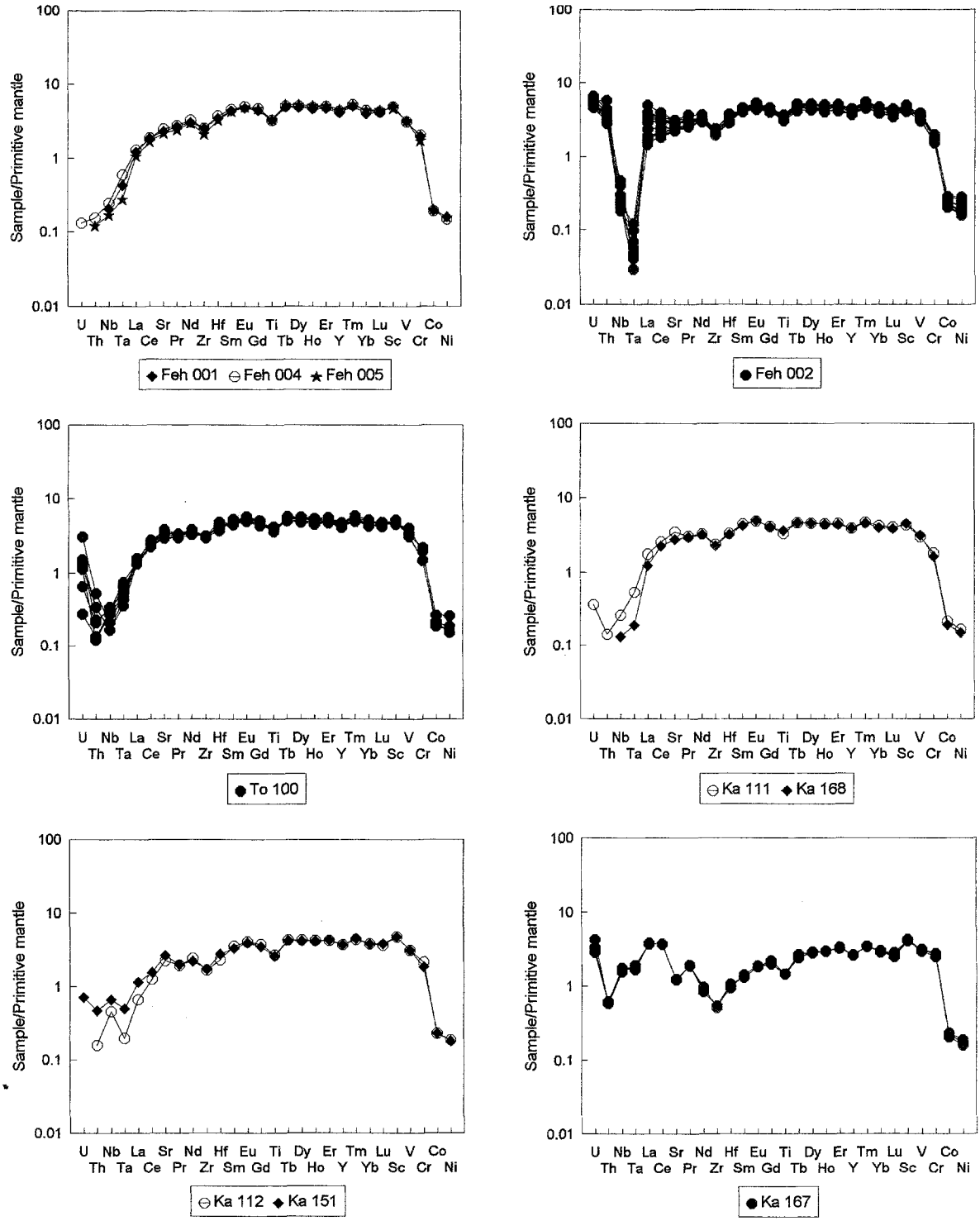

Fig. 3. Primitive mantle-normalized trace element patterns of clinopyroxenes from lherzolites and the harzburgite Ka 167 from the Graz Basin. Primitive mantle values are from *Sun* and *McDonough* (1989). The rocks labelled *Feh, To* and *Ka* are from Fehring, Tobaj and Kapfenstein, respectively. Elements are arranged according to increasing compatibility from left to right

and Ta = 0.007–0.02 ppm. The primitive mantle normalised concentration of Nb is lower than that of Ta in samples *Feh 001, Feh 004, Feh 005, To 100, Ka 111* and *Ka 168* and higher in *Ka 112* and *Ka 151*. The clinopyroxene from sample *Feh 002* has an extremely low Ta content (around 0.003 ppm which is 0.06 times primitive mantle).

Th and U abundances are low in samples *Feh 001, Feh 004* and *Feh 005* (Fig. 3) and they follow the decreasing trend defined by incompatibility, i.e., their primitive mantle-normalized abundances decrease almost continually from Sm toward U. The contents of U and Th are highly elevated in the clinopyroxene of *Feh 002*, where the abundances of these elements can exceed the primitive mantle-normalized abundances of the REEs (Fig. 3). The absolute values on average correspond to 0.12 ppm for U and 0.32 ppm for Th. The variation of Th in the clinopyroxenes of sample *Feh 002* shows a positive correlation with the variation of La (the correlation coefficient, $R^2 = 0.85$ for 11 spot analyses). Time resolved signals of Th and U indicate that both elements are hosted by the clinopyroxene (Fig. 4). Clinopyroxene from *To 100 has v*ariable and elevated U and weakly correlated but less elevated Th contents.

The trace element pattern of the clinopyroxene from harzburgite *Ka 167* is different from those described previously (Fig. 3). It has slightly lower HREE abundances (2–3 times primitive mantle) than the lherzolites. It shows a continuous decrease in elemental abundances with increasing incompatibility up to Zr and thereafter significant enrichment in the LREEs. Negative anomalies of Ti and Sr are present relative to the neighbouring REEs. The Nb and Ta content of the clinopyroxene of harzburgite *Ka 167* are significantly elevated relative to the other samples, they can reach up to 1.5 times primitive mantle values which correspond to Nb = 1.1 ppm and Ta = 0.07 ppm, respectively. The clinopyroxene of sample *Ka 167* is significantly enriched in U (almost 4 times primitive mantle) as compared to other incompatible elements.

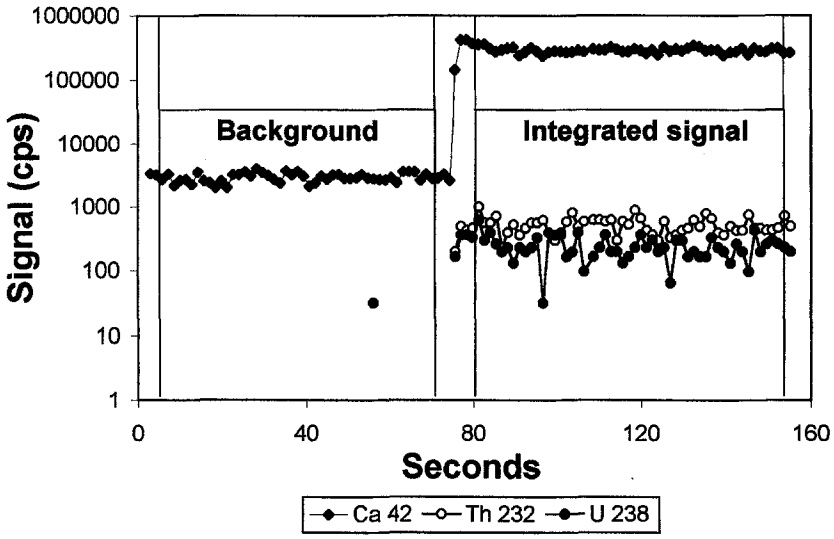

Fig. 4. Time-resolved signal (in cps) of Th, U and Ca (internal standard) in the clinopyroxene of lherzolite *Feh 002*. Both, Th and U, appear to reside in the clinopyroxene

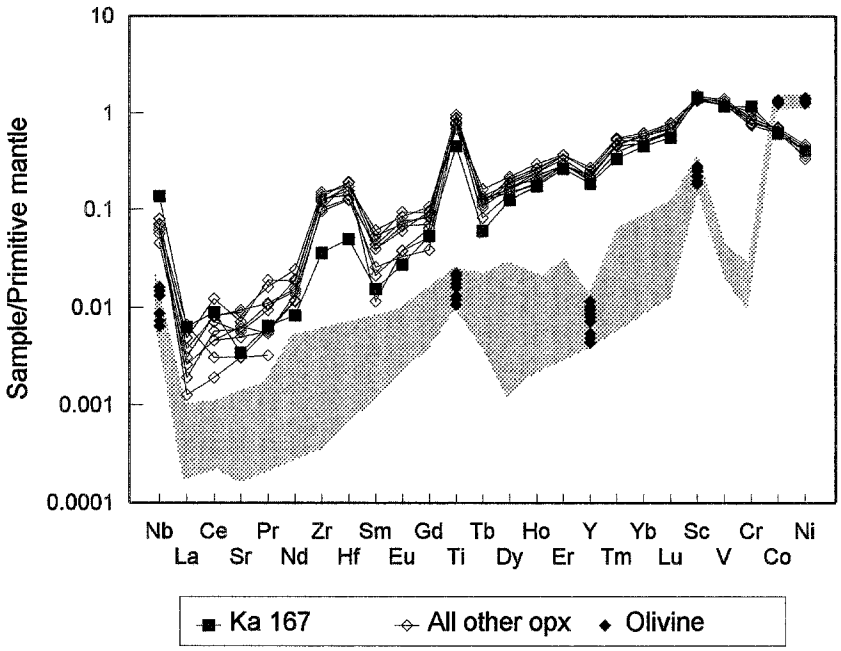

Fig. 5. Primitive mantle-normalized trace element patterns of orthopyroxenes and olivines in the lherzolites and the harzburgite Ka 167 from the Graz Basin, Styria. Normalized trace element patterns of olivines are represented by the shaded area. Only data for Nb, Ti and Y in olivines are individually plotted

The primitive mantle-normalized trace element patterns of orthopyroxenes show a continuous decrease from Lu to La with strong positive anomalies at Ti, Zr, Hf and Nb (Fig. 5). The abundances of Yb and Lu are approximately 0.5 times those of the primitive mantle whereas the abundance in La is below 0.006 times primitive mantle. Y and Sr have approximately the same normalized abundances as the neighbouring REEs. The primitive mantle-normalized trace element pattern of the orthopyroxene from the *Ka 167* harzburgite differs from that of the other orthopyroxenes (Fig. 5) in having significantly lower Zr and Hf contents, whereas its Nb content is almost double the Nb content of the lherzolite orthopyroxenes (0.09 ppm in *Ka 167* and 0.04–0.05 ppm in the other rocks).

The abundances of incompatible elements in the olivines (Fig. 5) are generally an order of magnitude lower than in the orthopyroxenes. Because the data have large errors and scatter, no individual analyses are reported for REEs, Zr and Sr in Table 2 and only the general primitive mantle-normalized concentration area is given for olivines. The Nb, Ti and Y contents of olivines have higher absolute values than all other elements and therefore more accurate analyses were obtained which are projected in Fig. 5. The general shape of the incompatible element patterns of the olivines is similar to that of the orthopyroxenes; Ti and Zr do not show any abundance anomaly but a significant positive anomaly for Nb is present in all olivines (Fig. 5).

Discussion

It is generally believed that the primitive mantle-normalized trace element pattern of clinopyroxenes in anhydrous spinel peridotites approximately reflects the trace element pattern of the whole rock. It may thus be used to identify depletion and enrichment processes in the lithospheric mantle, as well as to characterize its composition and evolution (*Downes* and *Dupuy*, 1987; *Salters* and *Shimizu*, 1988; *Lee* et al., 1996; *Blusztajn* and *Shimizu*, 1994; *Witt-Eickschen* and *Kramm*, 1997). However, orthopyroxene is also an important host for high field strength elements (HFSEs) such as Ti and Zr (*Rampone* et al., 1991; *McDonough* et al., 1992) and this must be taken into account in the interpretation of the clinopyroxene trace element pattern, especially in the interpretation of the anomalies of HFSEs (*McDonough* and *Frey*, 1989; *McDonough* et al., 1992).

Our results on minerals from the southeastern Austrian upper mantle peridotites generally confirm previous findings. Clinopyroxene is the major host for REEs, Y and Sr, containing over an order of magnitude larger amounts of these elements than orthopyroxene and two orders of magnitude more than olivine. However, the significant positive anomalies of Ti, Zr, Hf and Nb in orthopyroxene (Fig. 5) suggest that this mineral also plays some role in the whole rock HFSE budget in upper mantle peridotites. According to a very rough estimate based on averages of peridotite modes and mineral compositions, orthopyroxene contains 33% of the Ti and 10% of the Zr and Hf of the whole rock. The positive Ti, Zr and Hf anomalies in orthopyroxene cannot compensate the small negative anomalies relative to adjacent REEs displayed by these elements in the clinopyroxene trace element patterns. Thus the shape of the whole rock primitive mantle-normalized trace element pattern between La and Lu will be somewhat smoother but otherwise essentially the same as that of the clinopyroxene.

Not only orthopyroxene but also olivine shows a significant positive anomaly of Nb relative to LREEs in the primitive mantle-normalized trace element diagrams (Fig. 5). A similar enrichment of Nb in olivine was reported by *Ionov* et al. (1995) and by *Sun* and *Kerrich* (1995) from spinel lherzolite xenoliths from southeastern Siberia (Sikhote-Alin) and southeastern British Columbia, respectively. The Nb concentration in olivine measured by *Sun* and *Kerrich* (1995) is even more than an order of magnitude higher than in our olivines (0.19–0.26 ppm vs. 0.004–0.01 ppm). Due to its very low Nb content, olivine is probably not an important host for Nb (and for other incompatible trace elements) in spinel peridotites in spite of being the dominant rock-forming mineral.

Clinopyroxenes of all lherzolites have flat primitive mantle-normalized trace element patterns with slight LREE depletion which indicates that the lherzolites are residues after small degrees of partial melting of a chondritic primitive mantle. The low Cr-numbers in spinels and the high Al_2O_3 and Na_2O contents of pyroxenes are also in agreement with only a moderate depletion in "basaltic component".

The monotony in textures accompanying the simple and primitive geochemical character was established by *Kurat* et al. (1980, 1991) and *Vaselli* et al. (1996) for peridotites from the Kapfenstein locality. The geochemical data for xenoliths from the two additional localities from the Graz Basin area, Fehring and Tobaj, confirm that the upper mantle beneath the westernmost edge of the Pannonian Basin is

undisturbed and unfractionated. This is in sharp contrast to the extensively tectonized and metasomatized upper mantle beneath the central areas of the basin (*Embey-Isztin* et al., 1989; *Kurat* et al., 1991; *Downes* et al., 1992). According to recent models (*Embey-Isztin* et al., 1989, 1990) there is a diapiric upwelling of the upper mantle beneath the Pannonian Basin with the Graz Basin area lying on the eastern periphery of the mantle diapir. Thus, the lithospheric mantle under this region is essentially untectonized in contrast to the internal regions of the Pannonian Basin (*Kurat* et al., 1991; *Vaselli* et al., 1996).

However, the abundances of highly incompatible trace elements in some of the peridotites are not consistent with such simple findings. Only the clinopyroxenes of *Feh 001*, *Feh 004*, *Feh 005* and probably also *Ka 168* show continuously decreasing primitive mantle-normalized trace element abundances from La to U (Fig. 3). This decreasing trend corresponds to the order of increasing incompatibility and indicates loss of these elements by extraction of a partial melt or a fluid. The highly incompatible trace element patterns of the clinopyroxenes form the remaining spinel lherzolites (*Feh 002, To 100, Ka 112* and *Ka 151*) are "disturbed" (Fig. 3). Their unusual elemental abundances suggest that also processes other than partial melting or fluid extraction were operative during their history.

In peridotites that have clinopyroxenes with "undisturbed" Nb and Ta abundances (which means that the abundances of these elements are controlled only by extraction of partial melts/fluids) the primitive mantle-normalized Nb abundance is lower than that of Ta because Nb is more incompatible in clinopyroxene than Ta (*Green* et al., 1989; *Jenner* et al., 1994). However, the opposite trend can be seen in samples *Ka 112, Ka 151* and *Feh 002* where the normalized Nb concentration of clinopyroxenes is higher than that of Ta (Fig. 3). The Nb/Ta ratio varies between 7 and 13 in the clinopyroxenes of the "normal" peridotites, while this ratio is significantly higher in samples *Ka 151* (Nb/Ta = 24), in *Ka 112* (Nb/Ta = 43) and *Feh 002* (Nb/Ta = 85). The high Nb/Ta ratios in the clinopyroxenes of peridotites *Ka 112* and *Ka 151* are the result of their elevated Nb contents relative to the other samples while the high Nb/Ta ratio in the *Feh 002* lherzolite apparently is the result of its very low Ta content (Table 2).

Both Nb and Ta have very low concentrations in clinopyroxenes of upper mantle peridotites, so the possibility of analytical error should also be discussed. Because all data given in the Tables are the averages of at least five individual spot analyses, a possible control for the precision of the analysis is to investigate the standard deviations of the measurements. Apart from the *Feh 002* sample, the relative standard deviations ($\pm 2\sigma$) are below 25% for both elements. Typical examples are *Ka 111* ("normal" Nb/Ta) in which Nb = 0.17±0.030 ppm and Ta = 0.02± 0.0036 ppm, and *Ka 151* ("disturbed" Nb/Ta) where Nb = 0.43± 0.044 ppm and Ta = 0.018±0.0033 ppm. The relative standard deviations of the measured Nb and Ta concentrations in the Feh 002 clinopyroxene are larger, 35% for Nb and 48% for Ta. However, the standard deviations for the Nb and Ta measurements are far below the differences which cause these very contrasted Nb/Ta ratios in the clinopyroxenes in the different samples. Consequently, the "disturbed" Nb and Ta abundances in some peridotites are not an analytical artifact.

Previously it was believed that the Nb/Ta ratios of basalts and peridotites are relatively constant and nearly chondritic (*Jochum* et al., 1986, 1989; *Sun* and

McDonough, 1989) and the variation of Nb/Ta ratios in peridotitic xenoliths was attributed to poor data quality (*McDonough*, 1990). However, more recent results (*Rudnick* et al., 1993; *Ionov* et al., 1993, 1995) show that Nb/Ta ratios can be fractionated in mantle rocks by specific enrichment processes. An interaction with a metasomatizing agent having high Nb/Ta ratios could be an explanation for the unusually high Nb/Ta ratios in the clinopyroxenes of *Ka 112, Ka 151* and *Feh 002* xenoliths. The strong depletion of Ta in the lherzolite *Feh 002* could be the result of an extraction event (via partial melt or fluid) prior to the metasomatism event. Carbonatite melt/fluid is a possible candidate for the metasomatizing agent because it can be enriched in Nb relative to Ta which would lead to high Nb/Ta ratios (*Green* et al., 1992; *Ionov* et al., 1993). Although the high Nb/Ta ratios of upper mantle peridotites from Southeastern Austria may indicate a carbonatite metasomatism, the other indicators of interaction with carbonatite liquids or fluids (high Zr/Hf and Sr/Sm ratios, as well as high Sr, Ba, Rb and LREE contents) are missing in these rocks.

The variable enrichment of the highly incompatible elements U and Th in the clinopyroxenes of some Graz Basin peridotites further indicates cryptic metasomatism. Some peridotites like *To 100* are enriched mainly in U while others like *Feh 002* are enriched in both, U and Th. The inhomogeneous distribution of these elements in clinopyroxenes *Feh 002* and *To 100* indicates that equilibrium was not achieved during this process. This indicates that metasomatic enrichment has taken place relatively shortly before volcanic eruption. Correlation between the La and Th in clinopyroxene of *Feh 002* suggests that the enrichment of Th-U and LREEs are the result of the same metasomatic event. It remains open whether this event also brought the enrichment of Nb relative to Ta, or not. High Th and U abundances accompany the high Nb/Ta ratio in lherzolite *Feh 002* and maybe also in *Ka 151* but not in lherzolite *Ka 112*, where the highly fractionated Nb/Ta ratio is not accompanied by elevated U and Th abundances.

Lherzolite Ka 111 contains traces of Al rich and K-poor amphibole in equilibrium with the major phases indicating a H_2O-bearing metasomatising agent (*Kurat* et al., 1980, 1991). It is inferred that no trace elements were presumably carried by the water because no deviation in the trace element patterns of the bulk rock and the major minerals from those of non-metasomatized lherzolites could be detected. Our data confirm these findings but in addition show a small enrichment of the clinopyroxene of Ka 111 in U relative to Th and Nb (Fig. 3). This enrichment could be the result of the almost pure water metasomatism event. We can speculate that the concerted enrichment of U and Th in clinopyroxenes of lherzolites Ka 112, Ka 151 and *Feh 002* could be the result of a metasomatism by a CO_2-rich fluid that was also delivering LREEs and Sr and Nb in some cases.

Harzburgite sample *Ka 167* shows a two-stage evolution: a strong depletion caused by partial melting followed by cryptic metasomatism. The low abundances of primitive mantle-normalized HREEs in the clinopyroxene and the relatively steep decrease of the trace element abundances from HREE to Zr (Fig. 3) suggest a much more efficient extraction event for the *Ka 167* harzburgite than was experienced by the previously discussed lherzolites. The low modal abundance of clinopyroxene as well as the higher Cr-number of the spinel in this rock is also consistent with a high degree of elemental extraction. The enrichment of the clinopyroxene in LREEs

(especially La and Ce), Sr, Nb and Ta is very likely the result of a metasomatic event. In spite of the strong enrichment of Nb and Ta in clinopyroxene, the Nb/Ta ratio remains unfractionated (Fig. 3). The depletion and enrichment of elements in this rock can also be observed in the abundances of HFSE in orthopyroxene. It has significantly lower Zr and Hf and higher Nb contents than the orthopyroxenes of the lherzolites (Fig. 5). This sample is similar to samples described from other locations (e.g., *Kurat* et al., 1991, 1993; *Downes* et al., 1992) and is a typical example of an upper mantle zone that has seen high degrees of mass exchange in both ways, extraction and addition of incompatible elements.

Because of the LREE, Nb and Ta enrichment of clinopyroxene and orthopyroxene and the inhomogeneity in some of the clinopyroxenes, the metasomatic agent could be a precursor to the alkali basalt volcanism in the region. Alkali basalt volcanism took place between 1.5–2.5 Ma and before this happened and during the volcanic period the lithospheric mantle beneath the Graz Basin was possibly flushed by fluids. Metasomatic fronts moving ahead of the thermal diapir that created the Pannonian Basin may have been the ultimate cause of the alkali basalt volcanic activity in that region. That the metasomatism may occasionally involve water-dominated fluids is an unexpected conclusion; it would be worthwhile to search for the possible source(s) of that water.

Conclusions

Laser ablation microprobe ICP-MS is a powerful tool for the investigation of the minerals of upper mantle xenoliths. It permits analysis of elements such as U, Th, Nb, Ta and Hf that are present at ppb levels in mantle minerals and, therefore, are rarely analyzed because of analytical problems. This is especially true for trace elements in orthopyroxene and olivine. Our data confirm that orthopyroxene has significant positive anomalies in the abundances of HFSEs including Ti, Zr, Hf and Nb relative to the adjacent REEs in their primitive mantle-normalized trace element patterns and that olivine has a similarly high positive anomaly of Nb relative to LREEs.

The LREE-depleted trace element patterns suggest that the vast majority of the upper mantle peridotites, not only from the Kapfenstein area but from the two other localities as well, are residues after extraction of incompatible elements in either small fraction partial melts or trace element-rich fluids. The data from two additional localities from the Graz Basin area confirm that the upper mantle is generally untectonized and has a primitive chemical composition beneath the western edge of the Pannonian Basin adjacent to the mantle diapir. However, some of these peridotites show signs of interaction with one or more metasomatic fluids which affected only their highly incompatible trace elements. Possibly, CO_2-rich and, occasionally, also water-rich fluids were involved. The effect of these metasomatic events can be important because they can result in unusually high U and Th contents of the clinopyroxene accompanied by minor changes in the abundances of trace elements that are less incompatible than La. Moreover, this cryptic metasomatism could have significantly changed the Nb/Ta ratio of the clinopyroxenes in the upper mantle peridotites and this variation is not accompanied by changes of the other trace element contents.

Non-equilibrium trace element distributions in the clinopyroxene of some lherzolites strongly suggest that the metasomatic events took place shortly before the rocks were picked up by the alkali basalt magma and delivered to the Earth's surface. It is conceivable that metasomatism was caused by fluids that moved ahead of the thermal plume that created the Pannonian depression and that ultimately gave rise to the alkali basaltic volcanism. The common zones of enhanced mass exchange in the upper mantle are represented in our sample by one harzburgite which shows the strongest depletion as well as the strongest enrichment of incompatible elements of all our samples. However, rocks of that kind are rare in the border zone of the Pannonian basin as compared to the central region (e.g., *Embey-Isztin* et al., 1989; *Kurat* et al., 1991; *Downes* et al., 1992).

Acknowledgments

G. Dobosi's work at Memorial University was sponsored by a NATO postdoctoral fellowship and in Hungary by an OTKA 025978 grant. *G. Kurat* and *F. Brandstätter* are supported by FWF and the Austrian Academy of Sciences in Austria. Operation of the LAM-ICP-MS facility at Memorial University is supported by an NSERC Major Facilities Access Award. Additional research costs in this work are supported by an NSERC grant to *G.A. Jenner*. The *To 100* xenolith sample was collected by *W. Richter*. Thanks to *P. Hoppe*, MPI Mainz, for providing the unpublished SIMS data and *M. Tubrett* for assistance in LAM-ICP-MS analysis. The constructive criticism of two *Mineralogy and Petrology* reviewers is gratefully acknowledged.

References

Balogh K, Ebner F, Ravasz Cs, Herrmann P, Lobitzer H, Solti G (1994) K/Ar Alter tertiärer Vulkanite der südöstlichen Steiermark und des südlichen Burgenlandes. Jubiläumsschrift 20 Jahre Geologische Zusammenarbeit Österreich – Ungarn, Teil 2, S 55–72 (Wien)

Blusztajn J, Shimizu N (1994) The trace element variations in clinopyroxenes from spinel peridotite xenoliths from southwest Poland. Chem Geol 111: 227–243

Downes H, Dupuy C (1987) Textural, isotopic and REE variations in spinel peridotite xenoliths, Massif Central, France. Earth Planet Sci Lett 82: 121–135

Downes H, Embey-Isztin A, Thirlwall MF (1992) Petrology and geochemistry of spinel peridotite xenoliths from the western Pannonian Basin (Hungary): evidence for an association between enrichment and texture in the upper mantle. Contrib Mineral Petrol 109: 340–354

Embey-Isztin A, Dobosi G (1995) Mantle source characteristics for Miocene-Pleistocene alkali basalts, Carpathian-Pannonian Region: a review of trace elements and isotopic composition. Acta Volcanol 7: 155–166

Embey-Isztin A, Kurat G (1996) Young alkali basalt volcanism from the Graz Basin to the Eastern Carpathians (abstract). Advances in Austrian-Hungarian Joint Geological Research, Occasional Pap Geol Inst Hungary 189: 159–175

Embey-Isztin A, Scharbert HG, Dietrich H, Poultidis H (1989) Petrology and geochemistry of peridotite xenoliths in alkali basalts from the Transdanubian Volcanic Region, West Hungary. J Petrol 30: 79–105

Embey-Isztin A, Scharbert HG, Dietrich H, Poultidis H (1990) Mafic granulite and clinopyroxenite xenoliths from the Transdanubian Volcanic Region (Hungary): implications for the deep structure of the Pannonian Basin. Mineral Mag 54: 463–483

Embey-Isztin A, Downes H, James DE, Upton BGJ, Dobosi G, Imgram GA, Harmon RS, Scharbert HG (1993) The petrogenesis of Pliocene alkali volcanic rocks from the Pannonian Basin, Eastern Central Europe. J Petrol 34: 317–343

Frey FA, Prinz M (1978) Ultramafic inclusions from San Carlos, Arizona: petrologic and geochemical data bearing on their petrogenesis. Earth Planet Sci Lett 38: 129–176

Fryer BJ, Jackson SE, Longerich HP (1995) The design, operation and role of the laser ablation microprobe coupled with an inductively coupled plasma mass spectrometer (LAM-ICP-MS) in the Earth Sciences. Can Mineral 33: 303–312

Green TH, Sie SH, Ryan CG, Cousens DR (1989) Proton microprobe-determined partitioning of Nb, Ta, Zr, Sr and Y between garnet, clinopyroxene and basaltic magma at high pressure and temperature. Chem Geol 74: 201–216

Green TH, Adam J, Sie SH (1992) Trace element partitioning between silicate minerals and carbonatite at 25 kbar and application to mantle metasomatism. Mineral Petrol 46: 179–184

Heritsch H (1967) Über die Magmenentfaltung des steirischen Vulkanbogens. Contrib Mineral Petrol 15: 330–344

Horn I, Hinton RW, Jackson SE, Longerich HP (1997) Ultra-trace element analysis of NIST SRM 616 and 614 using Laser Ablation Microprobe-Inductively Coupled Plasma-Mass Spectrometry (LAM-ICP-MS): a comparison with Secondary Ion Mass Spectrometry (SIMS). Geostand Newsletter 21: 191–203

Ionov DA, Dupuy C, O'Reilly SY, Kopylova MG, Genshaft YS (1993) Carbonated peridotite xenoliths from Spitzbergen: implications for trace element signature of mantle carbonate metasomatism. Earth Planet Sci Lett 119: 283–297

Ionov DA, Prikhod'ko VS, O'Reilly SY (1995) Peridotite xenoliths in alkali basalts from the Sikhote-Alin, southeastern Siberia, Russia: trace element signatures of mantle beneath a convergent continental margin. Chem Geol 120: 275–294

Jackson SE, Longerich HP, Dunning GR, Fryer BJ (1992) The application of laser ablation microprobe-inductively coupled plasma-mass spectrometry (LAM-ICP-MS) to in situ trace element determinations in minerals. Can Mineral 30: 1049–1064

Jenner GA, Foley SF, Jackson SE, Green TH, Fryer BJ, Longerich HP (1994) Determination of partition coefficients for trace elements in high pressure-temperature experimental run products by laser ablation microprobe-inductively coupled plasma-mass spectrometry (LAM-ICP-MS). Geochim Cosmochim Acta 58: 5099–5103

Jochum KP, Seufert HM, Spettel B, Palme H (1986) The solar-system abundances of Nb, Ta and Y and the relative abundances of refractory lithophile elements in differentiated planetary bodies. Geochim Cosmochim Acta 50: 1173–1183

Jochum KP, McDonough WF, Palme H, Spettel B (1989) Compositional constraints on the continental lithospheric mantle from trace elements in spinel peridotite xenoliths. Nature 340: 548–550

Kurat G (1971) Granat-Spinell-Websterit und Lherzolith aus dem Basalttuff von Kapfenstein, Steiermark. Tschermaks Mineral Petrogr Mitt 16: 192–214

Kurat G, Palme H, Spettel B, Baddenhausen H, Hofmeister H, Palme C, Wänke H (1980) Geochemistry of ultramafic xenoliths from Kapfenstein, Austria: evidence for a variety of upper mantle processes. Geochim Cosmochim Acta 44: 45–60

Kurat G, Embey-Isztin A, Kracher A, Scharbert HG (1991) The upper mantle beneath Kapfenstein and the Transdanubian Volcanic Region, E. Austria and W. Hungary: a comparison. Mineral Petrol 44: 21–38

Kurat G, Palme H, Embey-Isztin A, Touret J, Ntaflos T, Spettel B, Brandstätter F, Dreibus G, Prinz M (1993) Petrology and geochemistry of peridotites and associated vein rocks of Zabargad Island, Red Sea, Egypt. Mineral Petrol 48: 309–341

Lee DR, Halliday AN, Davies GR, Essene EJ, Fitton JG, Temdjim R (1996) Melt enrichment of shallow depleted mantle: a detailed petrological, trace element and isotopic study of mantle-derived xenoliths and megacrysts from the Cameroon Line. J Petrol 37: 415–441

Longerich HP, Jackson SE, Fryer BJ, Strong DF (1993) The laser ablation microprobe – inductively coupled plasma – mass spectrometry. Geosci Can 20: 21–27

McDonough WF (1990) Constraints on the composition of the continental lithospheric mantle. Earth Planet Sci Lett 101: 1–18

McDonough WF, Frey FA (1989) Rare earth elements in upper mantle rocks. In: *Lipin BR, McKay GA* (eds) Geochemistry and mineralogy of rare earth elements. Rev Mineral 21: 99–145

McDonough WF, Stosch HG, Ware NG (1992) Distribution of titanium and rare earth elements between peridotitic minerals. Contrib Mineral Petrol 110: 321–328

Mercier JC, Nicolas A (1975) Textures and fabrics of upper mantle peridotites as illustrated by basalt xenoliths. J Petrol 16: 454–487

Rampone E, Botazzi P, Ottolini L (1991) Complementary Ti and Zr anomalies in orthopyroxene and clinopyroxene from mantle peridotites. Nature 354: 518–520

Richter W (1971) Ariégite, Spinell-Peridotite und Phlogopit-Klinopyroxenite aus dem Tuff von Tobaj im südlichen Burgenland. Tschermaks Mineral Petrogr Mitt 16: 227–251

Rudnick RL, McDonough WF, Chappel BW (1993) Carbonatite metasomatism in the northern Tanzanian mantle: petrographic and geochemical characteristics. Earth Planet Sci Lett 114: 463–475

Salters VJM, Shimizu N (1988) World-wide occurrence of HFSE-depleted mantle. Geochim Cosmochim Acta 52: 2177–2182

Salters VJM, Hart SR, Pantó Gy (1988) Origin of Late Cenozoic volcanic rocks of the Carpathian Arc, Hungary. AAPG Mem 45: 279–292

Sun M, Kerrich R (1995) Rare earth elements and high field strength element characteristics of whole rocks and mineral separates of ultramafic nodules in Cenozoic volcanic vents of southeastern British Columbia, Canada. Geochim Cosmochim Acta 59: 4863–4879

Sun SS, McDonough WF (1989) Chemical and isotopic systematics of oceanic basalts: implications for mantle composition and processes. In: *Sounders AD, Norry MJ* (eds) Magmatism in the ocean basins. Geol Soc London Spec Publ, pp 313–345

Taylor SR, McLennan SM (1985) The continental crust: its composition and evolution. Blackwell Scientific, Oxford

Vaselli O, Downes H, Thirlwall MF, Vannucci R, Coradossi N (1996) Spinel-peridotite xenoliths from Kapfenstein (Graz Basin, Eastern Austria): a geochemical and petrological study. Mineral Petrol 57: 23–50

Witt-Eickschen G, Kramm U (1997) Mantle upwelling and metasomatism beneath Central Europe: geochemical and isotopic constraints from mantle xenoliths from the Rhön (Germany). J Petrol 38: 479–493

Authors' addresses: *G. Dobosi* and *G. A. Jenner*, Department of Earth Sciences, Memorial University of Newfoundland, St. John's, Newfoundland, Canada, A1B 3X5; *G. Kurat* and *F. Brandstätter*, Naturhistorisches Museum Wien, Mineralogisch-Petrographische Abteilung, Burgring 7, Postfach 417, A-1014 Wien, Austria